Nonlinear correction schemes for the phase 1 LHC insertion region upgrade and dynamic aperture studies

R. Tomás, M. Giovannozzi, and R. de Maria
CERN, Geneva, Switzerland
(Received 5 June 2008; published 21 January 2009)

The phase 1 LHC interaction region (IR) upgrade aims at increasing the machine luminosity essentially by reducing the beam size at the interaction point. This requires a total redesign of the full IR. A large set of options has been proposed with conceptually different designs. This paper reports on a general approach for the compensation of the multipolar errors of the IR magnets in the design phase. The goal is to use the same correction approach for the different designs. The correction algorithm is based on the minimization of the differences between the IR transfer map with errors and the design IR transfer map. Its performance is tested using the dynamic aperture as a figure of merit. The relation between map coefficients and resonance terms is also given as a way to target particular resonances by selecting the right map coefficients. The dynamic aperture is studied versus magnet aperture using recently established relations between magnetic errors and magnet aperture.

DOI: 10.1103/PhysRevSTAB.12.011002 PACS numbers: 29.20.db

I. INTRODUCTION

The design of the interaction region (IR) of a circular collider is one of the most critical issues for the machine performance. Many constraints should be satisfied at the same time and the parameter space to be studied is huge [1,2]. The strong focusing required to increase the luminosity generates large values of the beta functions at the triplet quadrupoles. This in turn enhances the harmful effects of the magnets' field quality on the beam dynamics. It is therefore customary to foresee a system of nonlinear corrector magnets to perform a quasilocal compensation of the nonlinear aberrations. This is the case of the nominal LHC ring, for which corrector magnets are located in the Q_1, Q_2, and Q_3 quadrupoles, the latter including nonlinear corrector elements.

The strategy for determining the strength of correctors was presented in Ref. [3] and is based on the compensation of those first-order resonance driving terms that were verified to be dangerous for the nominal LHC machine. The proposed approach is based on a number of assumptions that are valid for the nominal LHC machine, but not necessarily true for the proposed upgrade scenarios [4,5], such as perfect antisymmetry of the IR optics between the two beams circulating in opposite directions. Indeed, some LHC upgrade options may not respect the antisymmetry of the IR optics between the two beams and the set of dangerous resonances might not be the same as for the nominal LHC or even be different among the LHC upgrade options. Furthermore, it might be advisable to use a method that should take into account all possible sources of nonlinearities within the IR, such as the field quality of the separation dipoles and also collective beam effects like the long-range beam-beam interactions.

For these reasons a more general correction algorithm should be envisaged, thus allowing a direct and straightforward application to any of the upgrade options or, more generally, to any section of an accelerator. The proposed method is based in the analysis of the nonlinear transfer map for a given section of a particle accelerator. Therefore it is conceived for the design phase when the magnetic errors have been measured. For an experimental setting of the corrector circuits other methods have been proposed [6–9].

The essential details about the nonlinear effects of the elements comprised in the section of the machine under consideration are retained in the nonlinear transfer map over one turn. For this reason the one-turn transfer map was proposed as an early indicator of single-particle instability with a reasonable correlation with the dynamic aperture [10–12].

This method relies on the developments on normal form theory, e.g. [13], which have also been the basis of other local correction schemes in the past, e.g., Refs. [14,15], for the Superconducting Super Collider arcs or Ref. [16] for the Large Hadron Collider (LHC). Different free parameters to minimize the selected figure of merit as well as different observables to benchmark the effectiveness of the correction proposed, such as analytical and numerical smears or detuning with amplitude, were studied.

In the next sections the proposed method is described and some applications to phase 1 LHC upgrade layouts are given, including the analysis of the effectiveness of the methods using the dynamic aperture (DA) as a figure of

merit. An illustrative first-order relation between achromatic map coefficients and resonance terms is also given.

II. MATHEMATICAL BACKGROUND

The transfer map between two locations of a beam line is expressed in the form

$$\vec{x}_f = \sum_{jklmn} \vec{X}_{jklmn} x_0^j p_{x0}^k y_0^l p_{y0}^m \delta_0^n, \tag{1}$$

where $\vec{x}_f$ represents the vector of final coordinates $(x_f, p_{xf}, y_f, p_{yf}, \delta_f)$, the initial coordinates being represented with the zero subindex, and $\vec{X}_{jklmn}$ is the vector containing the map coefficients for the four phase-space coordinates and the momentum deviation δ, considered as a parameter. The MAD-X [17] program together with the polymorphic tracking code (PTC) [18] provide the computation of the quantities $\vec{X}_{jklmn}$ up to the desired order.

To assess how much two maps, X and X', deviate from each other, the following quantity is defined:

$$\chi^2 = \sum_{jklmn} \|\vec{X}_{jklmn} - \vec{X}'_{jklmn}\|, \tag{2}$$

where $\|\cdot\|$ stands for the quadratic norm of the vector. To disentangle the contribution of the various orders to the global quantity χ^2, the partial sum χ_q^2 over the map coefficients of order q is defined, namely,

$$\chi_q^2 = \sum_{j+k+l+m+n=q} \|\vec{X}_{jklmn} - \vec{X}'_{jklmn}\| \tag{3}$$

so that

$$\chi^2 = \sum_q \chi_q^2. \tag{4}$$

The definition of χ_q^2 can be easily extended to introduce weighting of the different terms, using characteristic distances and divergences to compute the weights or simply to select those terms of more relevance. The applications described in this paper have all equal weights for all terms.

Furthermore, χ_q^2 is split into a chromatic $\chi_{q,c}^2$ and achromatic $\chi_{q,a}^2$ contribution, corresponding to

$$\chi_{q,a}^2 = \sum_{j+k+l+m=q} \|\vec{X}_{jklm0} - \vec{X}'_{jklm0}\|. \tag{5}$$

It is immediate to verify that $\chi_q^2 = \chi_{q,c}^2 + \chi_{q,a}^2$. Throughout this paper only the achromatic part will be considered since it typically dominates the particle stability in circular machines.

A. Relation to resonance driving terms

This section gives an illustrative first-order relation between achromatic map coefficients and resonance driving terms. This allows comparing this new approach to other correction algorithms based on the minimization of important resonance terms. Eventually these relations could also be used to target particular resonances by minimizing the right collection of map coefficients. However, in practice MAD-X and PTC are used to provide the map coefficients to the desired order, including all feed-down and feed-up effects. Transverse coupling is assumed to be a perturbation however adequate coordinate transformations could take stronger coupling into account.

In the Hamiltonian formalism Eq. (1) is written as

$$\hat{x}_f = e^{:h:} M \hat{x}, \tag{6}$$

where h is the nonlinear Hamiltonian and M represents the linear transport and $\hat{x}$ is the normalized coordinates, i.e. $\hat{x} = x/\sqrt{\beta_x}$. The Hamiltonian h is expanded in the resonance driving terms as follows:

$$h = \sum_{jklm} h_{jklm} \xi_x^{+j} \xi_x^{-k} \xi_y^{+l} \xi_y^{-m}, \tag{7}$$

$\xi_x^{\pm}$ being the complex normalized coordinates,

$$\xi_x^{\pm} = \hat{x} \pm i\hat{p}_x. \tag{8}$$

Using the previous expressions into Eq. (6),

$$\hat{x}_f = e^{:h:} M \tfrac{1}{2}(\xi_x^- + c.c.) = \tfrac{1}{2} e^{:h:} (e^{-i\Delta\phi_x} \xi_x^- + \text{c.c.}) \tag{9}$$

where c.c. stands for complex conjugate and $\Delta\phi_x$ is the phase advance between the two locations. To expand this expression the two following properties are used:

$$[\xi_x^{+j}, \xi_x^-] = -2ij\xi_x^{+j-1}, \tag{10}$$

$$e^{:h:} \xi_x^- \approx \xi_x^- + [h, \xi_x^-], \tag{11}$$

obtaining

$$\hat{x}_f = e^{-i\Delta\phi_x} \left(\xi_x^- - i \sum_{jklm} j h_{jklm} \xi_x^{+j-1} \xi_x^{-k} \xi_y^{+l} \xi_y^{-m} \right) + \text{c.c.}$$

This equation is the equivalent to Eq. (1) but using resonance terms instead of map coefficients. Therefore to relate them it is enough to take the right derivatives to isolate the term of interest. For example,

$$\begin{aligned} X_{p0000}^x &= \frac{1}{p!} \frac{\partial^p x_f}{\partial x^p} \bigg|_{x=0} = \frac{1}{p!} \sqrt{\frac{\beta_{xf}}{\beta_x^p}} \frac{\partial^p \hat{x}_f}{\partial \hat{x}^p} \bigg|_{x=0} \\ &= \sqrt{\frac{\beta_{xf}}{\beta_x^p}} \sum_{q=0}^{p} \frac{1}{q!(p-q)!} \frac{\partial^p x_f}{\partial \xi_x^{-p-q} \partial \xi_x^{+q}} \bigg|_{\xi^{\pm}=0} \end{aligned} \tag{12}$$

which after some algebra yields

$$X_{p0000}^x = -ie^{-i\Delta\phi_x} \sqrt{\frac{\beta_{xf}}{\beta_x^p}} \sum_{r=0}^{p} r h_{r(p-r)00} + \text{c.c.} \tag{13}$$

This expression already captures the most important features of the relation between map coefficients and resonance terms. For example, the sextupolar map coefficient X_{20000}^x depends linearly on h_{3000} and h_{1200}, or the (3,0) and

(1,0) resonances, respectively. It can be proved that the coefficient X^x_{pq000} depends on the same terms as $X^x_{(p+q)0000}$. The number of resonances involved in the relation increases linearly with the order of the map coefficient. Therefore minimizing local map coefficients implies a minimization of a collection of resonances. Hence, this approach might be useful when the knowledge of the full accelerator is limited. For completeness a more general coupling map coefficient is given below as a function of resonance terms, showing the features already described:

$$X^x_{p0q00} = -ie^{-i\Delta\phi_x}\sqrt{\frac{\beta_{xf}}{\beta_x^p\beta_y^q}}\sum_{r=0}^{p}\sum_{s=0}^{q} rh_{r(p-r)s(q-s)} + \text{c.c.} \tag{14}$$

III. CORRECTION OF MULTIPOLAR ERRORS

A. Algorithm

The basic assumption is that the multipolar field errors of the IR magnets are available as the results of magnetic measurements. The ideal IR map X without errors is computed using MAD-X and PTC to the desired order and stored for later computations. Including the magnetic errors to the IR elements perturbs the ideal map. To cancel or compensate this perturbation, distributed multipolar correctors need to be located in the IR. Throughout this paper we assume adjacent correctors to the triplet quadrupoles. Corrector choice will be based on performance. The map including both the errors and the effect of the correctors will be indicated with X'. The corrector strength is determined by simply minimizing χ_q^2 for these two maps. For efficiency, the minimization is accomplished order by order (see, e.g., Ref. [19] for a description of the dependence of the various orders of the nonlinear transfer map on the nonlinear multipoles). In such an approach the sextupolar correctors are used to act on χ_2^2, the octupolar ones on χ_3^2, and so on.

The code MAPCLASS [20] already used in [21] has been extended to compute χ_q^2 from MAD-X output. The correction is achieved by the numerical minimization of χ_q^2 using any of the existing algorithms in MAD-X for this purpose.

B. Performance evaluation

The evaluation of the performance of the method previously described is carried out using two of the three layouts proposed for the upgrade of the LHC insertions (see, e.g., Refs. [2,4,5,22] for the details on the various configurations under consideration).

The field quality of the low-beta triplets is considered to follow the assumption reported in Ref. [23]. This implies that the various multiple components b_n, a_n given by

$$B_y + iB_x = 10^{-4}B_2\sum_{n=2}^{\infty}(b_n + ia_n)\left(\frac{x+iy}{R_{\text{ref}}}\right)^{n-1}, \tag{15}$$

TABLE I. Random part of the relative magnetic errors of the low-beta quadrupoles at 17 mm radius [24]. The components b_n and a_n stand for normal and skew multipolar errors, respectively.

Order	b_n [10^{-4}]	a_n [10^{-4}]
2	0.349 431	0.477 730
3	0.100 570	0.309 803
4	0.067 294	0.062 218
5	0.135 565	0.057 960
6	0.012 633	0.016 546
7	0.003 812	0.014 816
8	0.006 825	0.003 813
9	0.008 446	0.003 973

where B_x, B_y represents the transverse components of the magnetic field and B_2 the field at the reference radius R_{ref}, scale down linearly with the reference radius, taken at a given fraction of the magnet aperture ϕ, according to [23]

$$\sigma(b_n, a_n; \alpha\phi, \alpha R_{\text{ref}}) = \frac{1}{\alpha}\sigma(b_n, a_n; \phi, R_{\text{ref}}), \tag{16}$$

where $\sigma(b_n, a_n; \alpha\phi, \alpha R_{\text{ref}})$ stands for the random field components of order n and α represents any scaling factor of the magnet aperture and the reference radius. As a natural consequence, large-bore quadrupoles will feature a better field quality than smaller aperture ones. The multipolar components used for the simulations discussed in this paper are listed in Table I.

An example of the order-by-order correction is shown in Fig. 1 for the so-called low-$\beta_{\max}$ configuration [2,5,22]. A total of 60 realizations of the LHC lattice are used in the computations. It is worthwhile stressing that, even though the random errors are Gaussian distributed with zero mean and sigma given by the values in Table I rescaled to the appropriate value of the magnet aperture, the limited statistics used to draw the values for a single realization implies that in reality nonzero systematic errors are included in the simulations.

One corrector per IR side and per type (normal and skew component) is used. Different locations of the nonlinear correctors can be used for the minimization of χ_q^2. The configuration having the lowest χ_q^2 after correction is selected for additional studies (see the next section). The difference between a nonoptimized positioning and the best possible one is illustrated in Fig. 2. There, the results of the proposed correction scheme in the case of a symmetric configuration (see Refs. [2,4,22]) are shown. The configuration corresponding to the gray dots achieves slightly better corrections over the ensemble of realizations and therefore is selected for further studies. Both configurations use normal and skew sextupole and dodecapole correctors. The worse configuration uses correctors between Q_{2A} and Q_{2B} and between Q_{2B} and Q_3 while the better configuration uses correctors between Q_{2A} and Q_{2B}

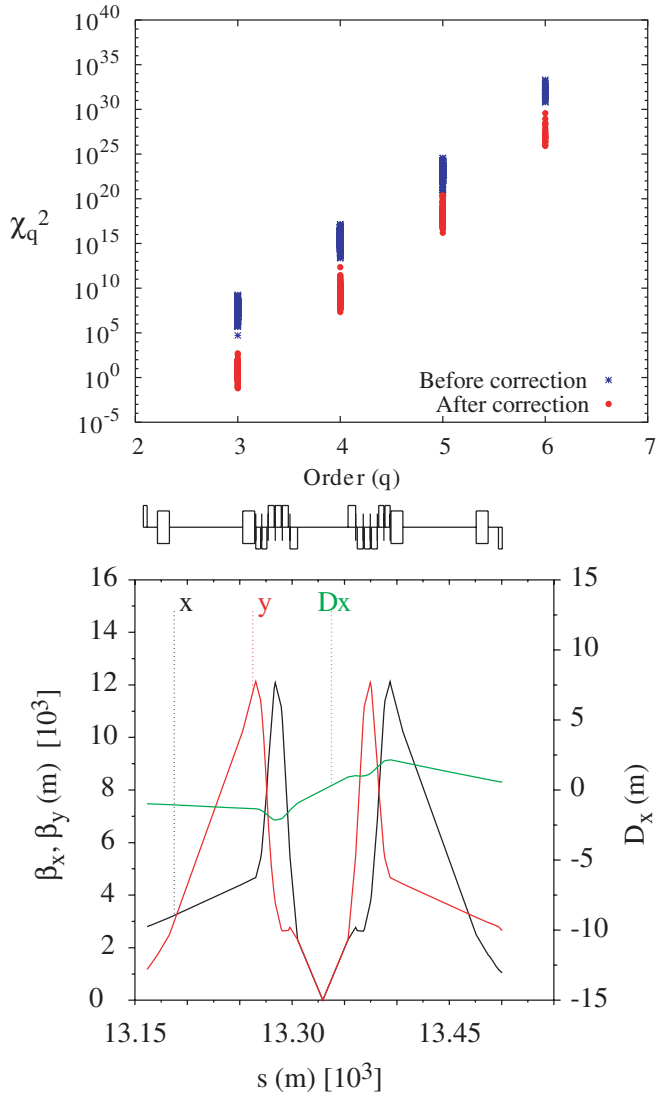

FIG. 1. (Color) Evaluation of the various orders of χ_q^2 (upper plot) before (blue markers) and after (red markers) correction. Sixty realizations of the random magnetic errors are used. The layout is the low-$\beta_{\max}$, whose optical functions are also reported (lower plot).

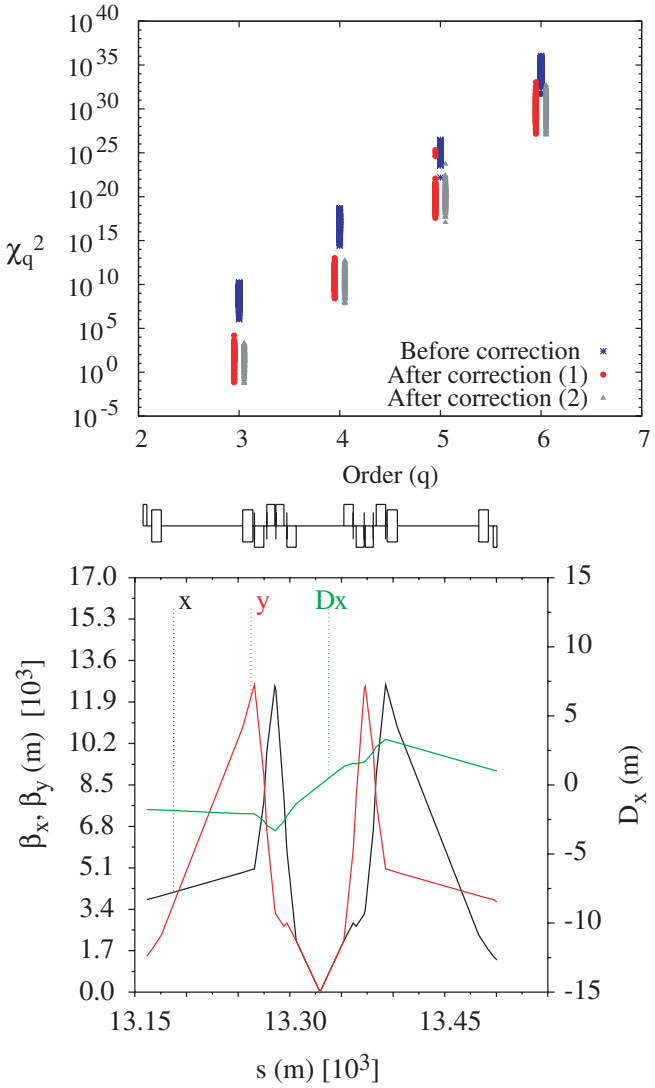

FIG. 2. (Color) Evaluation of the various orders of χ_q^2 (upper plot) before (blue markers) and after (gray and red markers) correction. The red markers represent a nonoptimized (in terms of correctors location) compensation scheme. Sixty realizations of the random magnetic errors are used. The layout is the symmetric one, whose optical functions are also reported (lower plot).

and after Q_3. Also the worse configuration required considerably larger strengths.

It is worth mentioning that the apertures of triplet magnets $Q_{2,3}$ of the two scenarios low-$\beta_{\max}$ and symmetric is 130 mm, while Q_1 is 90 mm for the low-$\beta_{\max}$ and 130 mm for symmetric.

IV. DYNAMIC APERTURE COMPUTATION

A. Assessment of the nonlinear correction algorithm

The main goal of the error compensation is to increase the domain in phase space where the motion is quasilinear, thus improving the single-particle stability. It is customary to quantify the stability of single-particle motion using the concept of dynamic aperture. The DA is defined as the minimum initial transverse amplitude becoming unstable beyond a given number N of turns. The standard protocol used to compute the DA for the LHC machine is based on $N = 10^5$ and a sampling of the transverse phase space (x, y) via a polar grid of initial conditions of type $(\rho\cos\theta, 0, \rho\sin\theta, 0)$ with $\theta \in [0, \pi/2]$. In practice, five values for θ are used. The scan in ρ is such that a 2σ interval is covered with 30 initial conditions. The momentum offset is set to 3/4 of the bucket height, which equals to 2.7×10^{-4} in relative momentum deviation at top energy. Even though the correction settings are computed for on-momentum particles, we still use the LHC standard

protocol, which includes an energy offset, since anyway DA is dominated by geometrical aberrations.

As far as the magnetic field errors used in the numerical simulations are concerned, the as-built configuration of the LHC is used. The information concerning the measured errors, as well as the actual slot allocation of the various magnets, is taken into account in the numerical simulations. The errors on the results of the magnetic measurements are included in the numerical simulations by adding random errors to the various realizations of the LHC ring. On the other hand, the field quality of the low-beta triplets from Table I and the scaling law from Ref. [23] are used. It is worth mentioning that the layouts under studies are not finalized, yet. In particular, the details for the implementation of the separation dipoles D_1 and D_2 are not fixed. As a consequence, no estimate concerning their field quality was taken into account in the modeling of the LHC ring. As for the evaluation of the correction schemes, sixty realizations of the random multipolar errors in the triplets are used and the value of DA represents the minimum over the realizations. The accuracy of the numerical computation of the minimum DA is considered to be at the level of $\pm 0.5\sigma$.

In Fig. 3 the DA for the two LHC upgrade options, low-$\beta_{\max}$ and symmetric, as a function of phase-space angle is plotted with and without nonlinear corrections schemes.

The correction algorithm proved to be particularly successful in the case of the symmetric layout. Indeed, for this configuration about 2.5σ are recovered thanks to the correction of the nonlinear b_3 and b_6 errors.

The improvement in the case of the low-$\beta_{\max}$ layout is less dramatic, as it allows recovering 2.5σ for small angles, only. It is also important to stress that the baseline DA is not the same for the two layouts, as the low-$\beta_{\max}$ is already well above 14.5σ without any correction. Furthermore, not only the optics is different for the options, but also the triplets' aperture. The first implies a different enhancement of the harmful effects of the triplets' field quality, while the latter has a direct impact on the actual field quality because of the scaling law [23]. Note that the case with larger DA, namely, low-$\beta_{\max}$, also features lower χ_q^2 values for all orders after correction, implying that this quantity might be a good indicator of particle stability. It is clear that the DA for the low-$\beta_{\max}$ is already well beyond the targets used for the design of the nominal LHC even without nonlinear correctors. The situation for the symmetric option is slightly worse and a correction scheme might be envisaged.

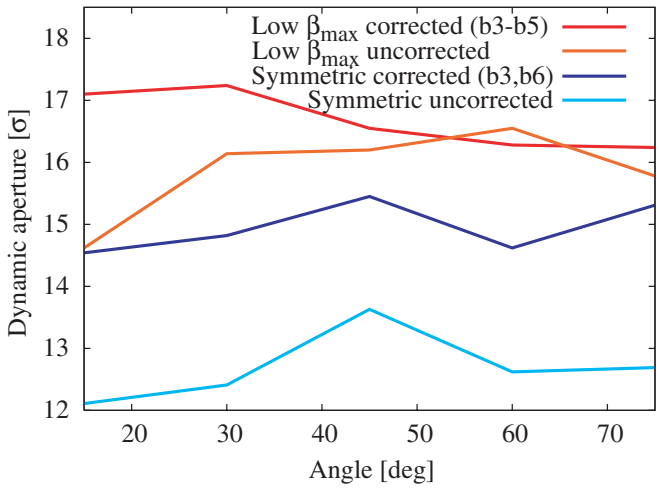

FIG. 3. (Color) Comparison of the minimum dynamic aperture for the LHC IR upgrade layouts low-$\beta_{\max}$ and symmetric with and without correction of the nonlinear magnetic errors in the low-beta quadrupoles.

B. Digression: Dynamic aperture vs low-beta triplet aperture

A third layout proposed as a candidate for the LHC IR upgrade is the so-called compact [2,5,22]. It features very large aperture triplet quadrupoles, namely, 150 mm diameter for Q_1 and 220 mm for Q_2 and Q_3. Thanks to the proposed scaling law, the field quality is excellent and the resulting DA is beyond 16σ. Hence, no correction scheme is required for this layout.

Nonetheless, a detailed study of the dependence of the dynamic aperture on the magnets aperture is carried out. The overall LHC model is the same as the one described in the previous sections, the main difference being the scan over the aperture of Q_1 and simultaneously over the apertures of Q_2 and Q_3. The optics is assumed to be constant, which implies that the configurations corresponding to larger magnets apertures than the nominal ones cannot be realized in practice.

The results are shown in Fig. 4. The minimum, average, and maximum (over the realizations) DA are shown for the two types of scans. The horizontal lines represent the asymptotic value of the DA and are obtained by using a huge (and unrealistic) value for the triplets aperture.

The dependence on the aperture of Q_1 is rather mild and an asymptotic value is quickly achieved. Furthermore, there exists a rather wide range of apertures for which the DA is almost constant. In particular, for $\phi > 110$ mm the asymptotic value of the DA is reached. A constant drop of DA is observed for $\phi < 100$ mm and, in general, the three curves behave the same.

The asymptotic value of DA for the scan of the Q_2 and Q_3 aperture is reached for apertures much larger than 280 mm. This is due to the larger value of the beta function in $Q_{2,3}$ than in Q_1, which enhance the impact of the quadrupoles' field quality on the beam dynamics. The spread between the asymptotic values for minimum, average, and maximum DA is smaller than for the case of the scan over the aperture of Q_1.

The way the asymptotic value is achieved is remarkably the same for both types of scans and was studied in more

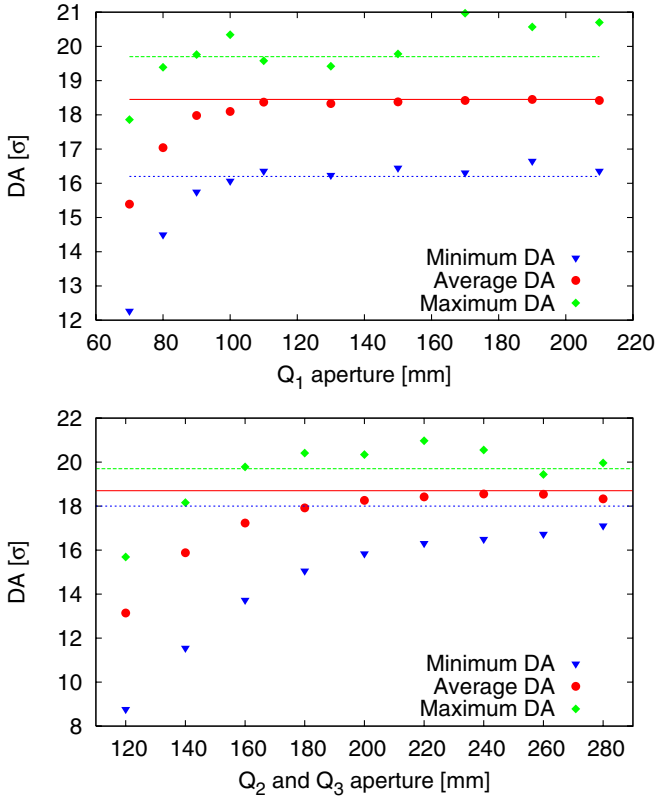

FIG. 4. (Color) DA as a function of the low-beta quadrupoles aperture. The scan over the aperture of Q_1 is shown in the upper plot (nominal aperture 150 mm), while Q_2 and Q_3 are considered in the lower plot (nominal aperture 220 mm). The layout is the so-called compact one.

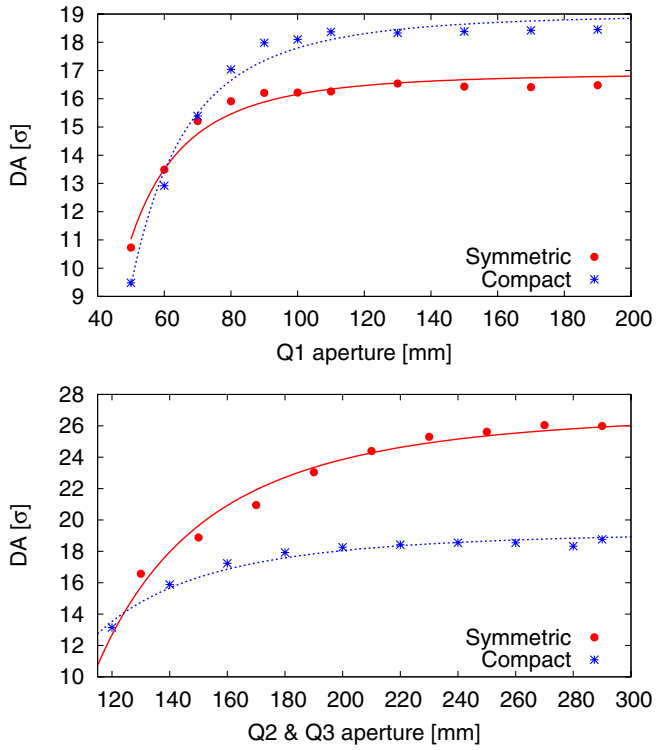

FIG. 5. (Color) Behavior of the average (over realizations) DA as a function of quadrupole apertures: (top) Q_1 and (bottom) Q_2 and Q_3. A fit of the function $f(\phi) = a\phi^{-3} + b$ is shown for all cases.

detail to assess whether it could be explained by a general scaling law. The hypothesis is that, due to the scaling law, Eq. (16), for high values of the magnets' aperture the lowest order multipole, i.e., the sextupolar one, dominates the beam dynamics. Therefore, the asymptotic behavior of the DA should scale inversely to the third power of the aperture ϕ. This hypothesis was applied not only to the compact layout, but also to the symmetric one, to ensure the independence of the conclusion on the details of the layout under study. To avoid the potential numerical instabilities related with the use of the minimum DA, the average of the realization was used for this study.

Figure 5 shows the DA for the two layouts and the two sets of quadrupole apertures together with a fit of the function $f(\phi) = a\phi^{-3} + b$. In all cases the inverse cubic asymptotic behavior seems to be in very good agreement with the numerical data. It is worth stressing that all the points shown in Fig. 5 were used for the computation of the fit curves. The asymptotic character of the scaling law implies that it should hold only for sufficiently large magnet apertures. This, indeed, explains why the agreement between the fit and the numerical data in the intermediate regime is not excellent (see Fig. 5, top).

V. CONCLUSIONS

A general algorithm for the correction of multipolar errors in a given section of a circular accelerator has been developed. It is based on the computation and comparison of map coefficients obtained from standard accelerator codes such as MAD-X and PTC. The algorithm aims at minimizing the difference between a target transfer map and the actual one. Both order-by-order and global optimization strategies are possible. Of course, the algorithm can be used also to optimize the location of the corrector elements. In its present form the nonlinear magnetic field errors are the only source of nonlinearities included in the transfer map. On the other hand, sources of nonlinear effects in the transfer map, such as beam-beam kicks from long-range encounters, could also be included in the correction algorithm. The efficiency of such an approach should be tested in practice with dedicated studies.

Direct relations between map coefficients and resonance terms have been computed. These relations could be used to extend the correction method to target specific resonances by selecting the right collection of map coefficients.

The correction algorithm was successfully tested on two layouts for the proposed IR upgrade of the LHC machine. The quality of the correction was also assessed by means of numerical simulations aimed at computing the dynamic

aperture. In the two cases under consideration, a sizable increase of the dynamic aperture due to the correction scheme is observed. Moreover, the case with larger DA also features lower χ_q^2 values for all orders implying that this quantity is a good indicator of particle stability.

In the numerical simulations used to evaluate the dynamic aperture, a new scaling law for the magnetic field errors as a function of the low-beta quadrupoles aperture was used. The impact of such an assumption on the value of the dynamic aperture was assessed in detail with a series of dedicated studies, where the triplets aperture is scanned. Smooth dependency of the dynamic aperture with respect to the magnets aperture is found, and a power law is fitted to the numerical data with very good agreement. These results could be used as an additional criterion for the definition of the required aperture of triplet quadrupoles. Indeed, one could derive the minimum aperture for which the dynamic aperture does not require any correction. Such a condition should then be taken into account together with the ones related to the needed beam aperture and energy deposition issues.

ACKNOWLEDGMENTS

We want to thank S. Fartoukh for many useful discussions. We also acknowledge the essential contribution in terms of computing power for the dynamic aperture evaluation from the LHC@home volunteers.

[1] M. Giovannozzi, "Optics Issues for Phase 1 and Phase 2 Upgrades," in Proceedings of CARE-HHH-APD Workshop on Interaction Regions for the LHC Upgrade, DAFNE, and SuperB, Frascati, Italy, 2007 (CERN-2008-006, CARE-Conf-08-001-HHH).

[2] R. de Maria, Phys. Rev. ST Accel. Beams **11**, 031001 (2008).

[3] O. Brüning, S. Fartouk, M. Giovannozzi, and T. Risselada, LHC-Project-Note 349, 2004.

[4] J.-P. Koutchouk, L. Rossi, and E. Todesco, LHC-Project-Report 1000, 2007.

[5] O. Brüning, R. de Maria, and R. Ostojic, LHC-Project-Report 1008, 2007.

[6] F. Pilat, Y. Luo, N. Malitsky, and V. Ptitsyn, in *Proceedings of the 21st Particle Accelerator Conference, Knoxville, 2005* (IEEE, Piscataway, NJ, 2005).

[7] R. Bartolini, I. Martin, G. Rehm, and J. Rowland, in *Proceedings of the 11th European Particle Accelerator Conference, Genoa, 2008* (EPS-AG, Genoa, Italy, 2008).

[8] R. Tomás, M. Bai, R. Calaga, W. Fischer, A. Franchi, and G. Rumolo, Phys. Rev. ST Accel. Beams **8**, 024001 (2005).

[9] G. Franchetti, A. Parfenova, and I. Hofmann, Phys. Rev. ST Accel. Beams **11**, 094001 (2008).

[10] M. Giovannozzi, W. Scandale, and E. Todesco, Part. Accel. **56**, 195 (1996).

[11] M. Giovannozzi, E. Todesco, A. Bazzani, and R. Bartolini, Nucl. Instrum. Methods Phys. Res., Sect. A **388**, 1 (1997).

[12] M. Giovannozzi, W. Scandale, and E. Todesco, Phys. Rev. E **57**, 3432 (1998).

[13] M. Berz, É. Forest, and J. Irwin, Part. Accel. **24**, 91 (1989).

[14] D. Neuffer and E. Forest, Phys. Lett. A **135**, 197 (1989).

[15] D. Neuffer, Part. Accel. **23**, 21 (1988).

[16] W. Scandale, F. Schmidt, and E. Todesco, Part. Accel. **35**, 53 (1991).

[17] H. Grote and F. Schmidt, Report No. CERN-AB-2003-024 ABP, 2003.

[18] E. Forest, F. Schmidt, and E. McIntosh, KEK Report No. 2002-3, 2002.

[19] A. Bazzani, G. Servizi, E. Todesco, and G. Turchetti, Report No. CERN-94-02, 1994.

[20] R. Tomás, Report No. CERN-AB-Note-017 ABP, 2006.

[21] R. Tomás, Phys. Rev. ST Accel. Beams **9**, 081001 (2006).

[22] F. Borgnolutti, O. Brüning, U. Dorda, S. Fartoukh, M. Giovannozzi, W. Herr, R. de Maria, M. Meddahi, E. Todesco, R. Tomás, and F. Zimmermann, in Proceedings of the 11th European Particle Accelerator Conference, Genoa, 2008, Ref. [7].

[23] B. Bellesia, J.-P. Koutchouk, and E. Todesco, Phys. Rev. ST Accel. Beams **10**, 062401 (2007).

[24] E. Todesco (private communication).